[11] Carrara, W. G., Goodman, R. S., and Majewski, R. M. (1995)
Spotlight Synthetic Aperture Radar—Signal Processing Algorithms, Boston: Artech House, 1995.

[12] Moreira, A., Scheiber, R., and Mittermayer, J. (1996)
Azimuth and range scaling for SAR and scan SAR processing.
In *Proceedings of IGARSS*, 1996, 1214–1216.

[13] Chen, V. C. (1998)
Time-frequency analysis of SAR image with ground moving targets.
In *Proceedings of SPIE'98, Vol. 3391*, Orlando, FL, Apr. 1998, 295–302.

[14] Xu, W., Chang, E. C., Kwoh, L. K., Lim, H., and Heng, W. C. A. (1994)
Phase-unwrapping of SAR interferogram with muti-frequency or multi-baseline.
In *Proceedings of IGASS'94*, 1994, 730–732.

[15] Schnitt, K., and Wiesbeck, W. (1997)
An interfermetric SAR processor avoiding phase ambiguities.
In *Proceedings of IGASS'97*, 1997, 1713–1715.

[16] Shnitkin, H. (1994)
Joint stars phase array radar antenna.
IEEE AES Magazine, (Oct. 1994), 34–41.

[17] Wood, J., and Barry, D. (1994)
Linear signal synthesis using the Radon-Wigner transform.
IEEE Transactions on Signal Processing, **42**, 8 (1994), 2105–2111.

[18] Cohen, L. (1995)
Time-Frequency Analysis.
Englewood Cliffs, NJ: Prentice-Hall, 1995.

[19] Qian, S., and Chen, D. (1996)
Joint Time-Frequency Analysis: Methods and Applications.
Englewood Cliffs, NJ: Prentice-Hall, 1996.

[20] Xia, X-G. (1999)
On estimation of multiple frequencies in undersampled complex valued waveforms.
IEEE Transactions on Signal Processing, **47** (Dec. 1999), 3417–3419.

[21] Zhou, G. C., and Xia, X-G. (1997)
Multiple frequency detection in undersampled complex-valued waveforms with close multiple frequencies.
Electronics Letters, **33**, 15 (July 1997), 1294–1295.

[22] Xia, X-G. (2000)
An efficient frequency determination algorithm from multiple undersampled waveforms.
IEEE Signal Processing Letters, (Feb. 2000).

[23] McClellan, J. H., and Rader, C. M. (1979)
Number Theory in Digital Signal Processing.
Englewood Cliffs, NJ: Prentice-Hall, 1979.

[24] Munson, D. C., Jr., O'Brien, J. D., and Jenkins, W. K. (1983)
A tomographic formulation of spotlight-mode synthetic aperture radar.
Proceedings of the IEEE, **71** (1983), 917–925.

[25] Fiedler, R., and Jansen, R. (2000)
Adventures in SAR processing.
Proceedings of SPIE, Orlando, FL, Apr. 2000.

[26] Bamler, R. (1992)
A comparison of range-Doppler and wave number domain SAR focusing algorithms.
IEEE Transactions on Geoscience and Remote Sensing **30** (July 1992), 706–713.

[27] Brown, W. M., and Fredricks, R. J. (1991)
Range-Doppler imaging with motion through resolution cells.
IEEE Transactions on Aerospace and Electronic Systems, **27** (Mar. 1991), 194–207.

[28] Soumekh, M. (1999)
Synthetic Aperture Radar Signal Processing with MATLAB Algorithms.
New York: Wiley, 1999.

[29] Soumekh, M. (1997)
Moving target detection in foliage using along track monopulse synthetic aperture radar imaging.
IEEE Transactions on Image Processing, **6**, 8 (Aug. 1997), 1148–1163.

Design of Frequency Modulated Waveforms via the Zak Transform

This paper introduces a new technique for designing frequency modulated waveforms that have ambiguity functions with desirable properties, such as strong peaking at the origin and low sidelobes. The methods employed involve signal design in Zak transform space, as well as the use of stationary phase arguments in the analysis of ambiguity functions.

I. INTRODUCTION. DEFINITIONS AND SOME PROPERTIES OF AMBIGUITY FUNCTION AND ZAK TRANSFORM

DEFINITION 1 The ambiguity function of a finite energy pulse $s(t)$ is a function of $s(t)$ given by the complex function of two variables [2]:

$$A_s(\tau,\nu) = \int_{-\infty}^{+\infty} s(t)\overline{s(t-\tau)}e^{-2\pi i\nu t}dt \qquad (1)$$

where $\overline{s(t)}$ denotes the complex conjugate of $s(t)$. The magnitude of the ambiguity function $|A(\tau,\nu)|^2$ is called the ambiguity surface.

The following are the main properties of the ambiguity function:

1) $A_s(0,0) = \|s\|^2$.

2) $|A_s(\tau,\nu)| < A_s(0,0)$, $(\tau,\nu) \neq (0,0)$, (maximum property).

3) Let $g(t) = s(t-x)e^{-2\pi iyt}$, then

$$A_g(\tau,\nu) = A_s(\tau,\nu)e^{-2\pi i(x\nu+y\tau)}.$$

4) $A_s(\tau,\nu) = \overline{A_s(-\tau,-\nu)}$, (symmetry property).

Manuscript received November 16, 2001; revised July 30, 2002 and February 19, 2003; released for publication November 10, 2003.

IEEE Log No. T-AES/40/1/826484.

Refereeing of this contribution was handled by S. S. Chornoboy.

5) $\int_{-\infty}^{+\infty}\int_{-\infty}^{+\infty}|A_s(\tau,\nu)|^2 d\tau\, d\nu = |A_s(0,0)|^2$ (volume property).

DEFINITION 2 For a given parameter $\alpha \geq 0$, the Zak transform $Z_\alpha f$ of f is the function on R^{2d} defined by

$$Z_\alpha f(x,y) = \sum_{k\in Z^d} f(x-\alpha k)e^{-2\pi i\alpha k y}. \tag{2}$$

A recent book by Gröchenig [8] gives a very good overview of contemporary Time-Frequency analysis. In the 'Zak Transform' chapter he says:

> The Zak transform was first introduced and used by Gelfand [5] for a problem in differential equations. Weil [10] defined this transform on arbitrary locally compact abelian groups with respect to arbitrary closed subgroups... . Subsequently, the Zak transform was rediscovered several times, notably by Zak [11], [12] for a problem in solid state physics and Brezin [3] for differential equations. In representation theory and in abstract harmonic analysis Z_α is often called the Weil-Brezin map, but in applied mathematics and signal analysis it has become customary to refer to Z_α as the Zak transform... . The popularity of the Zak transform in engineering seems largely due to Janssen's influential survey article [9].

In our work we use the Zak transform with $\alpha = 1$, $d = 1$, which for notational simplicity we denote by $Z_f(x,y)$. We state only those properties of the Zak transform we need. They are easily derived directly from the definition.

1) (Quasiperiodicity) $Z_f(x+p,y) = e^{-2\pi ipy}Z_f(x,y)$, and $Z_f(x,y+q) = Z_f(x,y)$, where p, q are arbitrary integers. Thus Z_f is completely determined by its values on the unit square $\Omega = [0,1]\times[0,1]$.

2) The cross ambiguity function $A_{f,g}(\tau,\nu)$ of signals $f(t)$ and $g(t)$ can be computed directly from the Zak transforms $Z_f(x,y)$ and $Z_g(x,y)$ [1]:

$$A_{f,g}(\tau,\nu) = \int_0^1\int_0^1 Z_f(x,y)\overline{Z_g(x+\tau,y+\nu)}e^{-2\pi ix\nu}dx\,dy. \tag{3}$$

3) The (auto) ambiguity function on the integer lattice is

$$A_f(n,m) = \int_0^1\int_0^1 |Z_f(x,y)|^2 e^{2\pi i(-mx+ny)}dx\,dy \tag{4}$$

so the $A_f(n,m)$s are basically the Fourier coefficients of the real, nonnegative function $|Z_f(x,y)|^2$.

II. WAVEFORM CONSTRUCTION

Consider the function

$$B_l(z) = e^{2l\pi i\|z\|_p} \tag{5}$$

where l is a positive real parameter, $z = (x,y) \in \Omega = [0,1]\times[0,1]$, and $\|z\|_p = (x^p + y^p)^{1/p}$. We can represent $B_l(z)$ as a Fourier series

$$B_l(z) = \sum_{n,m=-\infty}^{+\infty} b_{nm}^l e^{2\pi i(mx+ny)} \tag{6}$$

$$b_{nm}^l = \int_0^1\int_0^1 e^{2\pi iS}dx\,dy \tag{7}$$

where $S = l\|z\|_p - mx - ny$.

The major contribution to the value of the integral [4] arises from the immediate vicinity of the boundary and from the vicinity of those points at which S is stationary, and to the first approximation the contribution of stationary points, if there are any, is more important then the contribution of the end points. Stationary points are solutions of the system of equations:

$$0 = \frac{\partial S}{\partial x} = \frac{\partial}{\partial x}(l\|z\|_p - mx - ny) = \left(\frac{x}{\|z\|_p}\right)^{p-1}\cdot l - m \tag{8}$$

$$0 = \frac{\partial S}{\partial y} = \frac{\partial}{\partial y}(l\|z\|_p - mx - ny) = \left(\frac{y}{\|z\|_p}\right)^{p-1}\cdot l - n. \tag{9}$$

The system of equations (8) and (9) can be rewritten as

$$\begin{cases} m^{p'} = \dfrac{x^p}{\|z\|_p^p}\cdot l^{p'} \\ n^{p'} = \dfrac{y^p}{\|z\|_p^p}\cdot l^{p'} \end{cases}, \qquad \text{where} \quad p' = \frac{p}{p-1}.$$

Now, since $(m^{p'} + n^{p'})^{1/p'} = l\cdot((x^p/\|z\|_p^p) + (y^p/\|z\|_p^p))^{1/p'} = l$, the stationary points in Ω are located at

$$n \geq 0, \qquad m \geq 0, \qquad \|k\|_{p'} = l \tag{10}$$

where $k = (m,n)$, $1/p' + 1/p = 1$.

Equation (10) is a quarter of a circle in the $\mathbf{l}^{p'}$ norm. The coefficients b_{nm}^ls can be easily approximated as shown in the Appendix. The above analysis suggests that the largest Fourier coefficients lie on the circle of radius l in the $\mathbf{l}^{p'}$ norm. In order to test the accuracy of this, we have calculated the Fourier coefficients, using Matlab's 2-dimensional fast Fourier transform (FFT). The results confirm our earlier findings. Fig. 1 illustrates the results of the Matlab computations for $p = 2$, $l = \{10,50\}$. In these figures gray scale corresponds to the absolute value of the Fourier coefficients, with darker corresponding to larger. It is interesting to note that since the Fourier coefficients lie on the circle of radius l in the $\mathbf{l}^{p'}$ norm, the geometry of their locations in (n,m) space is l-invariant. We use this fact in the design of frequency modulated waveforms.

As is well known (and can be easily derived from the definition and basic properties of the Zak transform), if a Zak transform on the unit square happens to be given by a 2-variable trigonometric polynomial

$$Z_f(x,y) = \sum_m\sum_n b_{nm}^l e^{2\pi i(mx+ny)} \tag{11}$$

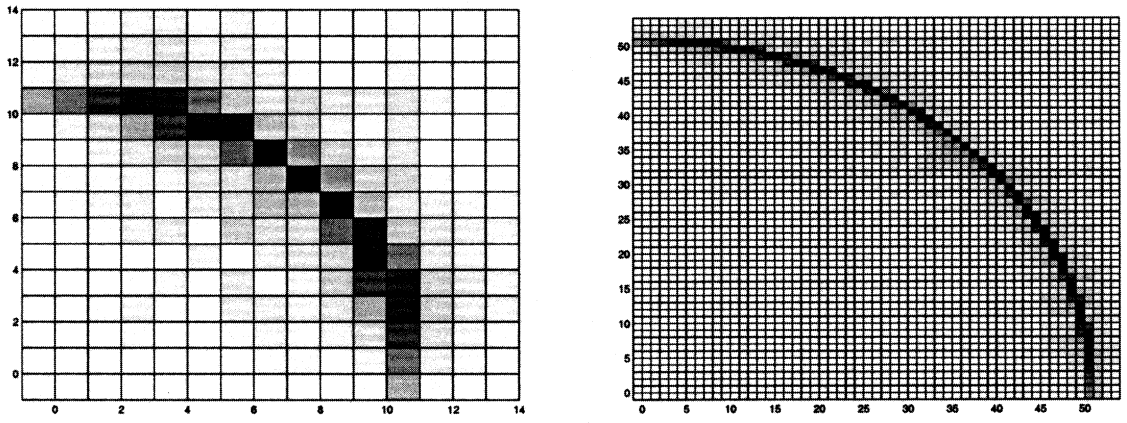

(a) (b)

Fig. 1.

which is then extended to the plane by quasiperiodicity, then the corresponding signal is a generalized pulse train

$$f(t) = \sum_{m,n} b^l_{nm} \chi_{[0,1]}(t-n) e^{2\pi i m t} \tag{12}$$

whose coefficients correspond in the indicated way to those of the trigonometric polynomial, and where $\chi_{[0,1]}$ is the indicator function of the unit interval.

In our previous work [6, 7], we used this correspondence of the coefficients to design families of frequency hopping waveforms with good ambiguity properties. Now we extend our result onto families of frequency modulated waveforms. As described in [7], if we choose the Zak transform $Z_f(x,y)$ of the signal $f(t)$ to be $\cos(2\pi l\sqrt{x^2+y^2})$ then the location of the sidelobes of the ambiguity surface is l-invariant, basically because the Fourier coefficients lie on a circle of radius l in the $\mathbf{l}^{p'}$ norm in (n,m) space, where in this case $p = 2$. As noted in [7] $\cos(2\pi l\sqrt{x^2+y^2})$ is one of a whole family of functions possessing this l-invariance property. l-invariance is a consequence of property 3 of the Zak transform and the ability to represent the square of the candidate Zak transform as a linear function of a rescaling of itself. The asymptotics of the previous section indicate that l-invariance holds for any linear combination of functions $e^{2\pi i l\|(x,y)\|_p}$. A simple and straightforward conclusion follows from the above analysis, namely that l-invariance and the volume property 5 of an ambiguity function together imply that increasing l lowers sidelobes. Another way to say this: the waveform corresponding to finer discretization (see Fig. 1) has ambiguity surface with lower sidelobes.

All of the above suggest the consideration of the continuous case, i.e., when n and m are not restricted to be integers. In that case (6) is not the Fourier series but a Fourier transform, and the pulse train (12) becomes an amplitude/frequency modulated waveform $f(t) = b^l(t)e^{2\pi i\theta^l(t)}$. The change in the amplitude is an undesired factor. For that reason we were tempted to consider the simpler case, when $b(t) = \text{const} = B$, i.e. a frequency modulated waveform

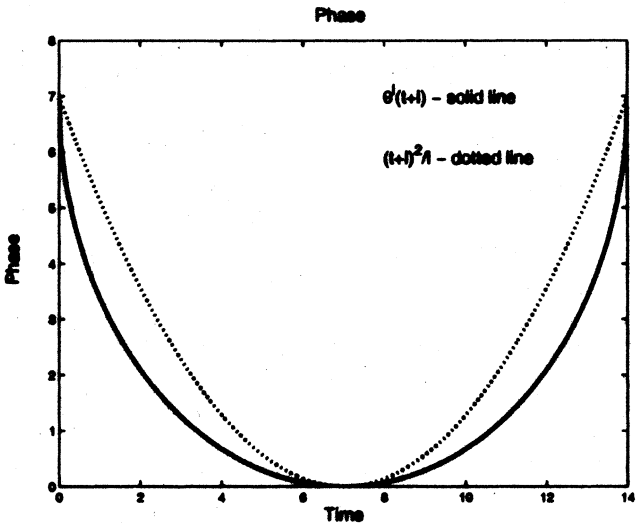

Fig. 2.

$$f(t) = Be^{2\pi i\theta^l(t)} \tag{13}$$

where $\theta^l(t) = l - (l^{p'} - t^{p'})^{1/p'}$ and $t \in [-l, l]$.

The phase $\theta^l(t+l)$, as well as the phase $(t+l)^2/l$ of the chirp signal are shown in Fig. 2. In this particular example $l = 7$ and $p = 2$. In general l is any positive real number which corresponds to the duration of the signal, and p is a positive real number that indicates the particular family of the frequency modulated waveforms. Fig. 3 represents the graph of an instantaneous frequency. In both figures the solid line corresponds to the described Non-linear FM waveform and the dashed line corresponds to the linear FM (LFM) waveform.

The real parts of the above waveforms are shown in Fig. 4. The time cross-sections of the ambiguity surface of our waveform (solid line), as well as the LFM signal (dashed line), are shown in logarithmic

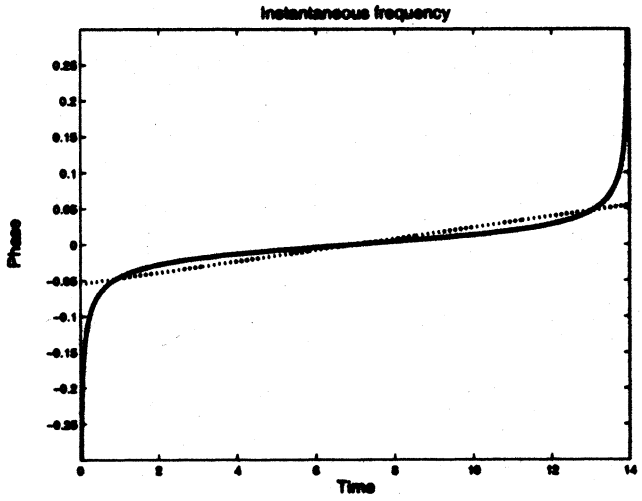

Fig. 3.

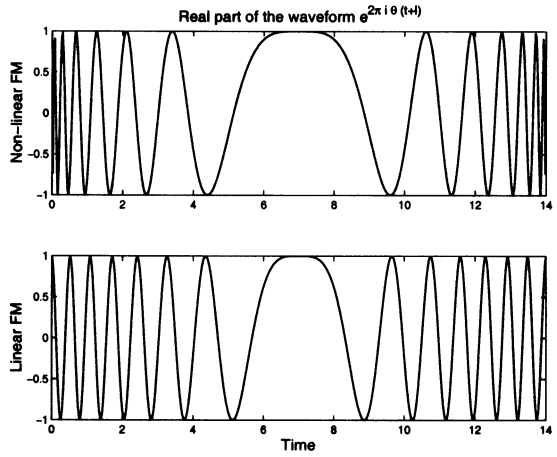

Fig. 4.

scale in Fig. 5. The number of sampling points used in the computations is 2^{10}.

The frequency cross sections of the ambiguity surface of our waveform (as well as any frequency modulated waveform $e^{i\theta(t)}$) is the same as the LFM signal. The ambiguity surface of our waveform is shown in Fig. 7. Because of the symmetry of the ambiguity surface with respect to the origin (property 4 of the ambiguity function), it is sufficient to display only the part of the surface where $\tau \geq 0$. It was chosen to plot $|A_s(\tau,\nu)|$ rather than $|A_s(\tau,\nu)^2|$, in order to emphasize the ridge along the instantaneous frequency without resorting to log scale. The ambiguity surface of the LFM signal $e^{(t+l)^2/l}$ is shown for comparison in Fig. 6.

III. CONCLUSION

We have introduced a new technique for designing frequency modulated waveforms. It is our intention, by introducing this method of waveform design via the Zak transform, to advance the design theory of signals having desired properties of the ambiguity function.

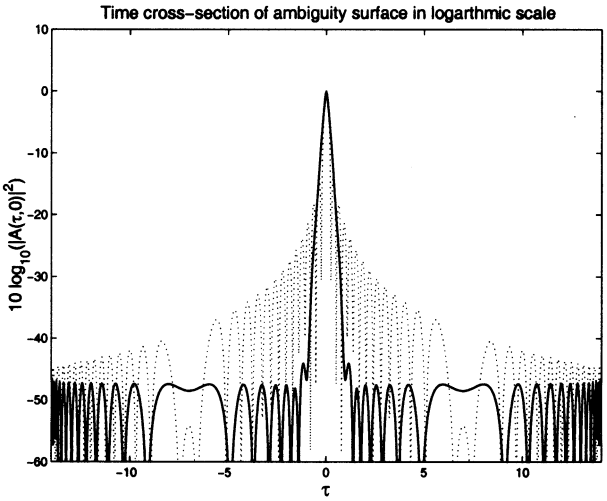

Fig. 5.

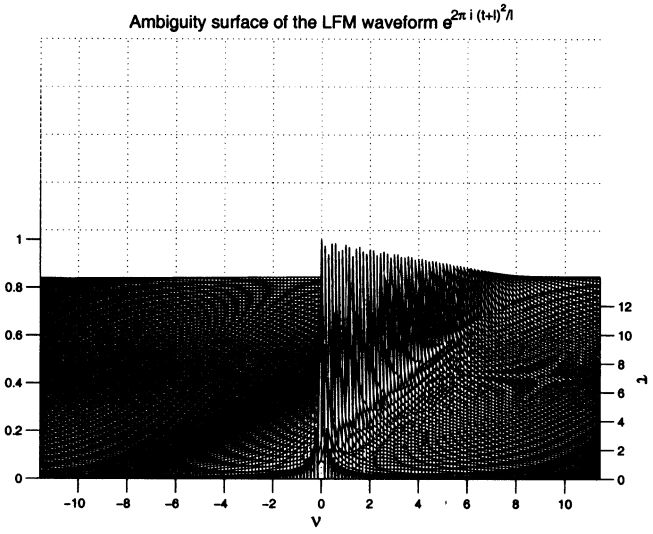

Fig. 6.

APPENDIX

The coefficients b^l_{nm}s can be easily approximated as shown below.

Note that the variables x and y can be interchanged in (6), therefore $b^l_{nm} = b^l_{mn}$, and thus we have to consider only one eighth of the circle, i.e., $0 \leq n \leq m$, $\|k\|_{p\prime} = l$. To compute the integral (7) we will first integrate with respect to the variable y, and then with respect to x, i.e.,

$$b^l_{nm} = \int_0^1 V(x)dx, \qquad V(x) = \int_0^1 e^{2\pi i S} dy. \quad (14)$$

The contributions V_0 and V_1 of the end points $y = 0$ and $y = 1$ to the last integral are well known [4] to be

$$V_0 = \frac{i + O(l^{-1})}{2\pi S_y(x,0)} e^{2\pi i S(x,0)} \quad (15)$$

$$V_1 = \frac{i + O(l^{-1})}{2\pi S_y(x,1)} e^{2\pi i S(x,1)} \quad (16)$$

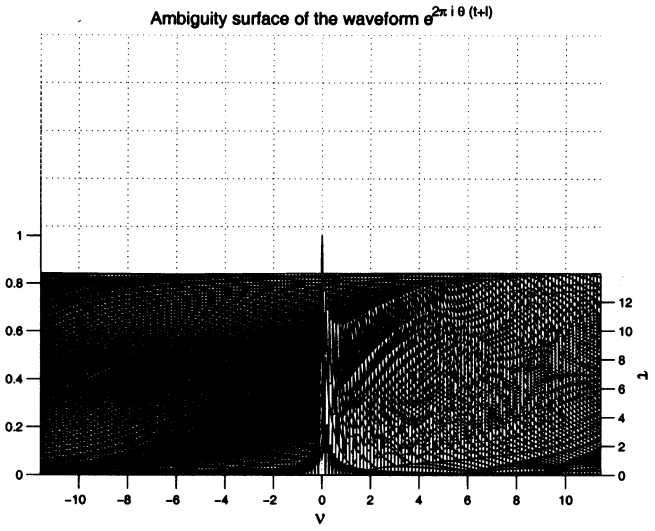

Fig. 7.

and [4] the contribution of the stationary point $y_{\text{stat}} = (n/m)^{1/(p-1)}$ is

$$V_{y_{\text{stat}}} = |S_{yy}(x, y_{\text{stat}})|^{-1/2} e^{2\pi i S(x, y_{\text{stat}}) + i\pi/4 + O(l^{-1})} \tag{17}$$

where $S_y = \partial S/\partial y$.

In our case $S(x, y_{\text{stat}}) = 0$, and

$$S_{yy}(x, y_{\text{stat}}) = mn\frac{p-1}{lx} \cdot \left(\frac{m^2}{ln}\right)^{1/(p-1)}. \tag{18}$$

Finally, after we integrate the contributions (15), (16), and (17) with respect to x, we will obtain

$$\int_0^1 V_{y_{\text{stat}}} dx = |S_{yy}(4/9, y_{\text{stat}})|^{-\frac{1}{2}} e^{i\pi/4} = O(l^{-1/2}) \tag{19}$$

$$\int_0^1 V_0 dx = \frac{1 - e^{2\pi i(l-m)}}{4\pi^2(l-m)} = O(l^{-1}) \tag{20}$$

$$\int_0^1 V_1 dx = O(l^{-3/2}). \tag{21}$$

We have not explicitly exhibited the m, n dependance in the above estimates, since l is the decisive parameter in our waveform design, because it controls the level of approximation to the continuous case. The value of b_{nm}^l is equal to the expression in (19) up to $O(l^{-1})$:

$$b_{nm}^l \approx \frac{3}{2}\left|mn\frac{p-1}{l} \cdot \left(\frac{m^2}{ln}\right)^{1/(p-1)}\right|^{-1/2} e^{i\pi/4}. \tag{22}$$

IRINA GLADKOVA
Dept. of Computer Science
CCNY
Convent Ave. & 138th St.
New York, NY 10031
E-mail: (gladkova@cs.ccny.cuny.edu)

REFERENCES

[1] Auslander, L., Geshwind, F., and Warner, F. (1995)
Radar waveform design and the Heisenberg group.
Applied and Computational Harmonic Analysis, **2** (1995), 350–362.

[2] Blahut, R. E. (1991)
Radar and Sonar, Part I.
New York: Springer-Verlag, 1991, ch. Theory of Remote Surveillance Algorithms.

[3] Brezin, J. (1970)
Harmonic analysis on manifolds.
Transactions on American Mathematical Society, **150** (1970), 611–618.

[4] Erdélyi, A. (1956)
Asymptotic Expansions.
New York: Dover, 1956.

[5] Gel'fand, I. M. (1950)
Eigenfunction expansions for equations with periodic coefficients.
Dokl. Akad. Nauk. SSR, **73** (1950), 1117–1120.

[6] Gladkova, I. (2001)
Families of waveforms with good auto and cross ambiguity properties.
In *Proceedings of the 2001 IEEE Radar Conference*, 138–140.

[7] Gladkova, I. (2001)
The Zak transform and a new approach to waveform design.
IEEE Transactions on Aerospace and Electronic Systems, **37**, 4 (2001), 1458–1464.

[8] Gröchenig, K. (2000)
Foundations of Time-Frequency Analysis.
Boston: Birkhäuser, 2000.

[9] Janssen, A. J. E. M. (1988)
The Zak transform: A signal transform for sampled time-continuous signals.
Philips Journal of Research, **43**, 1 (1988), 23–69.

[10] Weil, A. (1964)
Sur certains groupes d'opérateurs unitaires.
Acta Math., **111** (1964), 143–211.

[11] Zak, J. (1967)
Finite translations in solid state physics.
Phys. Rev. Lett., **19** (1967), 1385–1397.

[12] Zak, J. (1972)
The kq-representation in the dynamics of electrons in solids.
Solid State Physics, **27**, 1 (1972), 1–62.